

Preparation of Double Silver Mixed Interlayer Carbon Nanotube Cathode and Improvement of Electron Emission Performance in Wood Material Printing

Li Yu-kui^{1*}, Wang Wen-xiu¹, Yang Juan¹

¹School of electronic information engineering, Jinling Institute of Technology, Nanjing 211169, P. R. China

*Corresponding Author.

Abstract:

In order to improve the photochromic resistance of printed wood products, the preparation of double silver mixed interlayer carbon nanotube cathode in wood material printing was studied in this paper. A novel dual silver-mixing intermediate-layer carbon nanotube (DSMIL-CNT) cathode was fabricated on a horniness cathode faceplate. The silver-CNT composite electrode paste, which included numerous multi-walled CNTs, was printed on a transparent bar electrode to form a silver-CNT composite electrode with circular convex-shaped external edges. The particles-mixed CNT layer paste, containing many minute Ag particles, was sintered to form the particles-mixed CNT layer. The silver-CNT composite electrode and the particles-mixed CNT layer were placed between the transparent bar electrode and the top emitter layer. The CNTs on the top emitter layer were mainly utilized to emit electrons. Simple and feasible fabrication of DSMIL-CNT cathode adopted the reliable and low-cost screen-printing, baking, and sintering process. Using the DSMIL-CNT cathode, a flat panel display was fabricated to form the emission image. As compared to a common bar electrode CNT cathode, the tested DSMIL-CNT cathode possessed superior electron emission properties, stronger adhesion performance, and better emission current stability. The maximum electron emission current was 2915.7 μ A, and the largest fluctuation range of electron emission current did not exceed 1.2% in the testing course of 120 min. In the image testing, the emission image of DSMIL-CNT cathode possessed higher luminous brightness and better luminance uniformity than the common bar electrode one. The fabricated DSMIL-CNT cathode is considered lucrative for the commercialization of flat panel displays. It possesses considerable potential for practical applications due to its preparation simplicity, excellent performance, and low production cost.

Keywords: Cathode; Electron emission; wood material printing; Luminance uniformity; Stability

I. INTRODUCTION

Carbon nanotubes (CNTs) comprehensively combine high aspect ratio and good electric conductivity, making them lucrative for producing high-performance electron emitters with a stable emission current^[1-3]. In cathode applications, where CNTs are utilized to emit electrons, the screen-printing method is frequently applied as a conventional cathode fabrication process^[4-6]. The advantages of the screen-printing process over other cathode preparation techniques include larger cathode area fabrication, pattern cathode preparation possibility, and lower production costs^[7-9]. However, the electron emission performance of screen-printed CNTs is significantly deteriorated by a random distribution of CNTs in the cathode^[10-12]. Although the emission capability of CNTs can be improved via the adhesive taping method, the residual adhesive often leaves secondary contaminations on the treated CNTs^[13-15]. Alternatively, the plasma bombarding method can enhance the emission uniformity of CNTs, but the treatment procedure is too complex and expensive^[16-18]. For the mechanical rubbing method, the electron emission performance of CNTs could be perfected, yet the damaging to the CNT cathode usually occurred because of the direct contact on CNT cathode and the non-uniform rubbing force in the treatment course^[19-21]. Given this, more research efforts and alternative approaches to the CNT cathode improvement are topical^[22-25]. In this paper, a new dual silver-mixing intermediate-layer (DSMIL) CNT cathode is proposed and tested. The cathode structure design and the detailed description of the manufacturing process are presented. In the preparation course, the low-cost screen-printing, baking, and sintering process are employed, and the fabrication of a transparent bar electrode, silver-CNT composite electrode, particles-mixed CNT layer, and top emitter layer are also introduced. The emission image of the DSMIL-CNT cathode with high-performance luminous brightness and uniformity is achieved. The developed DSMIL-CNT cathode is considered an efficient approach to improving the electron emission performance of screen-printed CNTs.

II. EXPERIMENTAL

2.1 Preparation of printing paste

Multi-walled CNTs (produced by Timesnano, Chengdu Organic Chemicals Co., Ltd.) with the tube diameter exceeding 20nm were used in this study. Three types of printing pastes, namely: the silver-CNT composite electrode paste, the particles-mixed CNT layer paste, and the top emitter layer paste, were prepared. For silver-CNT composite electrode paste, the purified multi-walled CNTs, the original silver slurry, and a small amount of other organic solvents were mixed in a beaker to form the silver-CNT composite electrode mixture. Subsequently, the

silver-CNT composite electrode mixture was heated up to 85°C, while an appropriate amount of terpineol solvent was gradually added during the continued temperature-rise period from 85°C. After the stable heating temperature of 185°C was reached, the electromagnetic stirring process for the silver-CNT composite electrode mixture (together with the added terpineol solvent) was conducted until a smooth silver-CNT composite electrode paste was formed. For the particles-mixed CNT layer paste, the weighted Ag particles, multi-walled CNTs, and terpineol solvent were blended in another beaker to form a particles-mixed CNT layer mixture. The weight ratio of Ag particles and multi-walled CNTs was 0.5:1. Then, an electromagnetic stirring process was carried out for the particles-mixed CNT layer mixture. During the stirring process, an appropriate amount of ethylcellulose was added, and the heating process for the particles-mixed CNT layer mixture (together with the added ethylcellulose) was synchronous began at the same time. The maximum heating temperature was maintained at 96°C. The stirring process continued until the added ethylcellulose was entirely dissolved, and a slick particles-mixed CNT layer paste was achieved. Finally, the top emitter layer paste was also obtained with a similar preparation process of the particles-mixed CNT layer paste. The only difference was that the Ag particles were not included in the top emitter layer paste.

2.2 Fabrication of DSMIL-CNT cathode

A structural schematic diagram of the DSMIL-CNT cathode is depicted in Fig.1(a). Firstly, the cut soda-lime glass of a 2mm thickness was used as the horniness cathode faceplate. With the precise photo-etching process, the indium tin oxide film on the horniness cathode faceplate surface was divided to form the transparent bar electrodes. The silver-CNT composite electrode paste was screen-printed on the horniness cathode faceplate. A baking process was performed for the printed silver-CNT composite electrode paste in an automatic drying oven, in which the constant baking temperature was 223°C and the baking time was 30 min. Subsequently, the baked silver-CNT composite electrode paste on the horniness cathode faceplate was sintered in the sintering furnace. The corresponding sintering condition parameters were as follows: the nitrogen was utilized as shielding gas; the maximum sintering temperature was 559°C; the holding time at the maximum sintering temperature was 7 min; the whole sintering time was 72 min. Thus, the silver-CNT composite electrode were produced on the transparent bar electrode. Good electrical conduction was realized between one silver-CNT composite electrode and the corresponding transparent bar electrode. A structure schematic diagram of one silver-CNT composite electrode is illustrated in Fig.1(b). Silver-CNT composite electrodes were parallel-arranged on the horniness cathode faceplate, while both external edges of the silver-CNT composite electrode had a circular convex shape. Secondly, the particles-mixed CNT layer paste was printed on the silver-CNT composite electrode; a baking process for the printed particles-mixed CNT layer paste, and a sintering process for the baked particles-mixed CNT

layer paste were carried out in proper sequence. The corresponding manufacture parameters were identical to those of the silver-CNT composite electrode, including the baking and sintering temperatures, sintering time, etc. Thirdly, after the top emitter layer paste was prepared on the particles-mixed CNT layer, the top emitter layer was fabricated. The corresponding baking process for the printed top emitter layer paste and the sintering process for baked top emitter layer paste were also performed. The baking and sintering process parameters were adjusted and optimized. The typical fabrication process condition parameters were as follows: baking temperature of 185°C, baking time of 49 min, the maximum sintering temperature of 532°C, the total sintering time of 80 min, and holding time at the maximum sintering temperature of 10 min. A proper post-treatment process was conducted to improve the top emitter layer's electron emission capability, leading to the completion of the DSMIL-CNT cathode fabrication. For comparing the effects on the electron emission characteristics of different CNT cathodes, a common bar electrode CNT cathode was also fabricated, in which the top emitter layer was directly prepared on the transparent bar electrode of the horniness cathode faceplate.

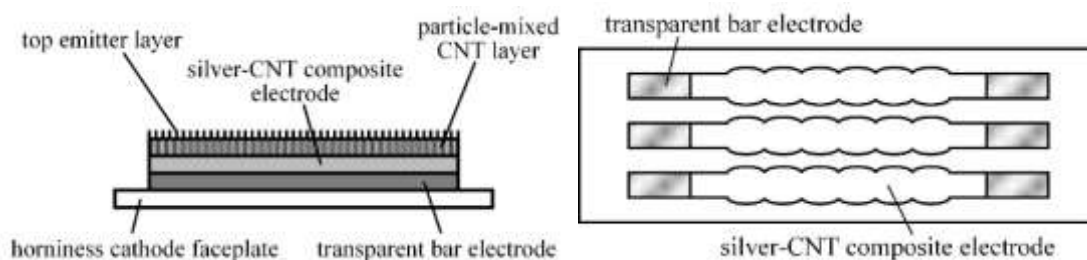


Fig 1: Structural schematic diagram of (a) the DSMIL-CNT cathode and (b) the silver-CNT composite electrode.

III. RESULTS AND DISCUSSION

3.1 Surface morphology of CNT cathode

The surface morphology of CNT cathode was observed with the scanning electron microscopy (SEM). The corresponding SEM photos of both types of CNT cathodes were obtained, as shown in Fig.2(a-d). The surface morphology of the baked DSMIL-CNT cathode is illustrated in Fig.2(a). As seen from Fig.2(a), there were many organic binder materials on the DSMIL-CNT cathode surface. Due to the strong viscosity of organic binders, many CNTs were glued together, of which the electron emission of CNT could be seriously obstructed. Meanwhile, many CNT ends were covered by binder materials and, thus, could not protrude

from the cathode surface. Even if the electric field intensity on the cathode surface was sufficient to emit electrons, these CNT ends were non-operational. Consequently, the organic binder materials needed to be removed. The surface morphology of the sintered DSMIL-CNT cathode is presented in Fig.2(b). After the sintering process, a clear CNT cathode surface was formed, as seen from the photo. In Fig.2(b), several facts can be observed. Firstly, a homogeneous CNT cathode surface was obtained, and many CNTs twined each other. So, more CNTs could take part in the normal electron emission. Secondly, there were many CNT ends on the CNT cathode surface, which generated additional sources of the electron emission. Due to the random distribution of CNT ends, the mutual interference of electron emission in different CNT ends disappeared. Thirdly, due to the top emitter layer's covering, no Ag particles in the particles-mixed CNT layer and the silver-CNT composite electrode could be observed. Therefore, the parasitical electron emission from minute Ag particles was avoided. Finally, in the preparation course of the DSMIL-CNT cathode, the sintering process was adopted in all experiments. The maximum sintering temperature for the top emitter layer of 532°C was maintained for 10 min. At such a high sintering temperature, the organic binder materials were rapidly vaporized and disappeared. The argon was employed as a shielding gas in the sintering course, which inhibited the re-deposition of organic binder materials or other impurities. Thus, the organic binder materials could be eliminated more thoroughly. The CNT could endure a high temperature exceeding 950°C, so all CNTs in the DSMIL-CNT cathode were preserved. Moreover, due to good argon shielding, CNTs of DSMIL-CNT cathode also were not oxidized in the sintering course.

Figure 2(c) depicts the surface morphology of baked common bar electrode CNT cathode. As seen in Fig.2(c), massive organic binder materials survived the baking process and kept obstructing the normal electron emission of CNTs. The comparative analysis of Fig.2(a) and Fig.2(c) revealed the following trends. Firstly, in the preparation course of CNT cathode, the baking process could be used as a pre-processing procedure of the sintering process, only relying on the baking process, the organic binder materials in CNT cathode paste could not be eliminated effectively. Secondly, the baking process was also an indispensable step for the preparation of CNT cathode. During the baking process, the aqueous organic solvent in paste would be prior cleaned. In the absence of the baking process's pre-processing procedure and direct conduction of the sintering process, numerous cracks would appear on the CNT cathode surface due to the possible anisotropic surface tension. Thirdly, for both types of CNT cathodes, the baking process was conducted, and the treated results were similar and satisfactory. Thus, the baking process was applicable and recommended for both types of CNT cathodes. The surface morphology of the sintered common bar electrode CNT cathode is depicted in Fig.2(d). As seen from the photo, after the sintering process, the common bar electrode CNT electrode also possessed a smooth cathode surface morphology. In the common bar electrode CNT

cathode, the top emitter layer was directly printed on the transparent bar electrode, while in DSMIL-CNT cathode, the top emitter layer was fabricated on the particles-mixed CNT layer. For both types of CNT cathode, CNTs in the top emitter layer were utilized to emit cathode electrons. Since the top emitter layers were identical, it was not surprising that the cathode surface morphology of the common bar electrode CNT cathode and the DSMIL-CNT cathode was similar. The organic binder materials were removed quite effectively, and a pure CNT layer remained. For both types of CNT cathodes, no floating CNTs were revealed in the CNT cathode surfaces, and all CNTs possessed a good adherence to the cathode surface. It was advantageous to enhance the adhesive performance of CNT and improve the electron emission capability of CNT, insofar as any separation of floating CNTs could cause the short circuit of CNT cathode and grid, which would directly lead to scraping of the flat panel display and hinder the normal electron emission of CNTs.

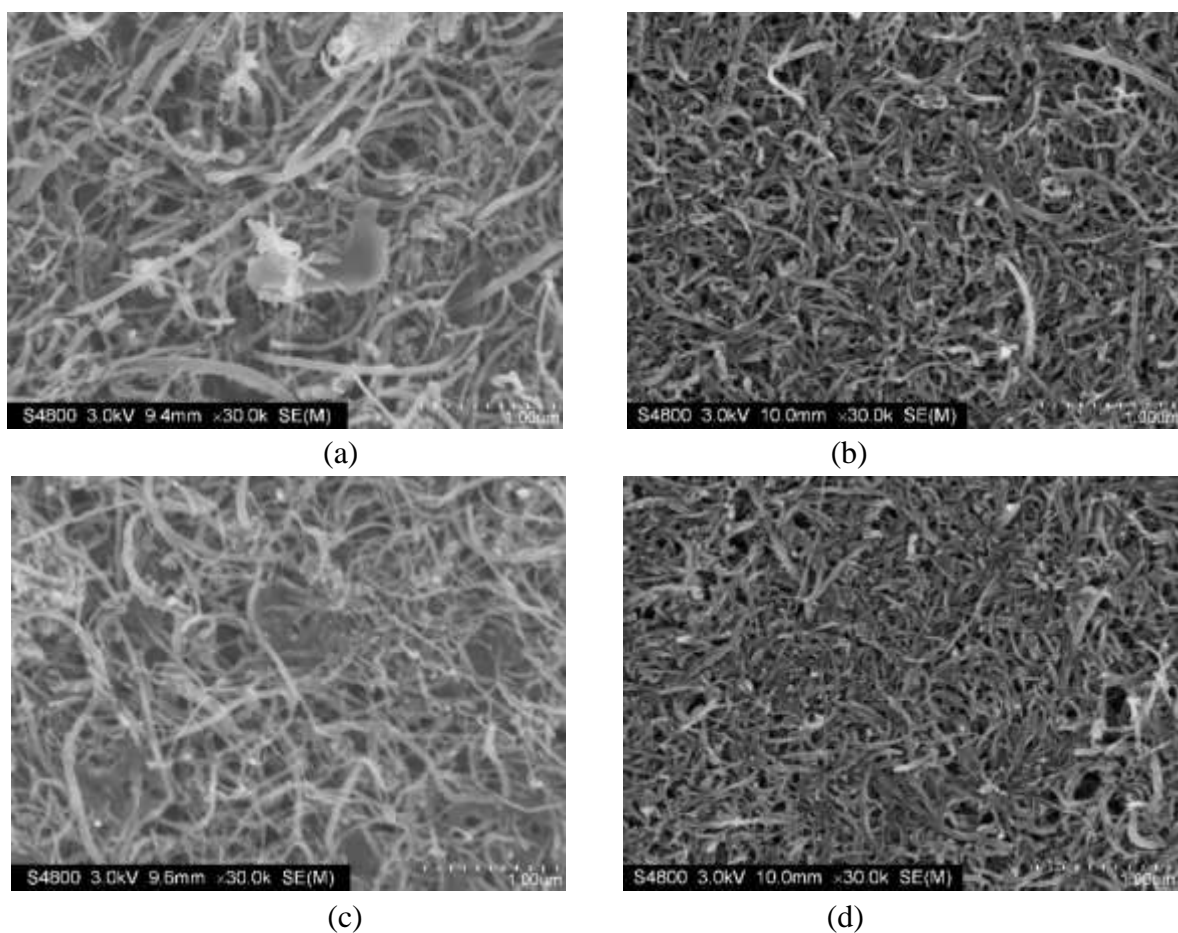


Fig 2: SEM photo of surface morphology for (a) baked DSMIL-CNT cathode, (b) sintered DSMIL-CNT cathode, (c) baked common bar electrode CNT cathode, and (d) sintered common

bar electrode CNT cathode.

3.2 Experimental curves of electron emission characteristics

For the in-depth study of electron emission characteristics, the integrated vacuum measuring system platform was employed for both types of CNT cathodes. The measured characteristics were obtained and plotted in Fig.3. The identical measuring conditions were used as follows: the DSMIL-CNT cathode and common bar electrode CNT ones were installed in the vacuum chamber of the integrated vacuum measuring system platform; the anode potential and grid potential were applied with different direct current (DC) electric sources on the experiment platform; the ammeters were used to monitor the electron emission current; the anode potential was fixed at 1.82kV and remained unchanged in the measuring course; the vacuum chamber pressure had the order of 10^{-4} Pa.

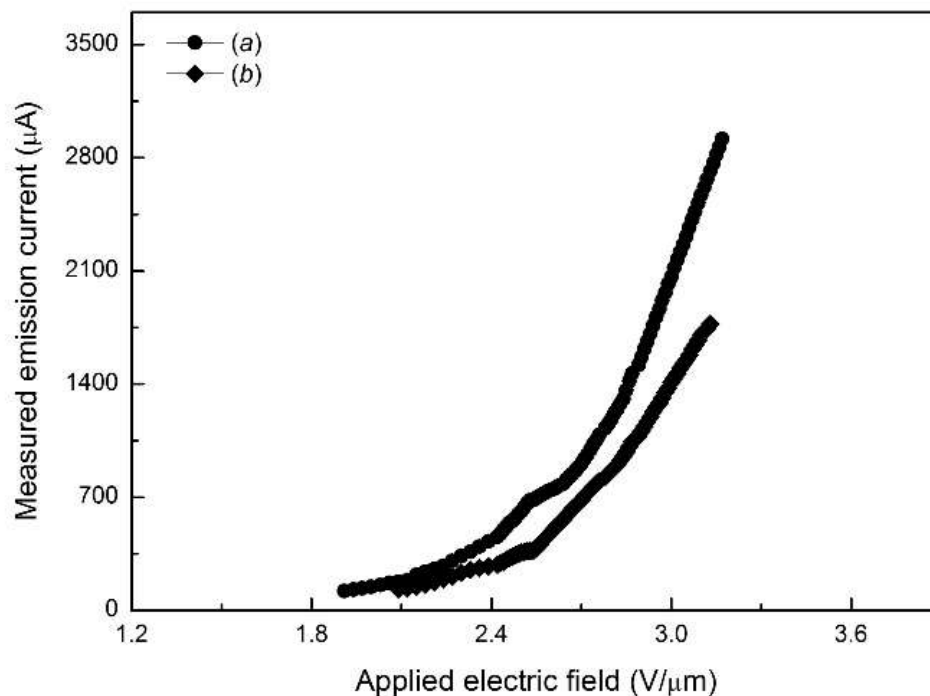


Fig 3: Experimental curves of electron emission characteristics for (a) the DSMIL-CNT cathode, and (b) the common bar electrode CNT cathode.

Firstly, according to the overall variation trends of the electron emission characteristic curves depicted in Fig.3, both types of CNT cathodes possessed a typical electron emission capability, which complied with the electron emission dynamic change rule of CNTs. For

example, when the electric field intensity was enhanced from 2.62 to 2.91V/ μm , the electron emission current of the DSMIL-CNT cathode was increased from an initial 763.5 to 1617.5 μA , while that of the common bar electrode CNT cathode also grew from an initial 526.8 to 1135.4 μA . The analysis shows that, in the DSMIL-CNT cathode, the silver-CNT composite electrode and the particles-mixed CNT layer possessed good cathode potential transferring performance. Thus, a strong electric field intensity was formed on CNT ends of the top emitter layer, and the CNT ends would be compelled to emit electrons into the vacuum. With the enhancement of applied electric field intensity, the number of cathode electrons provided by CNT ends would also be increased according to the “field emission” change rule. So it was natural that the cathode current would become larger. Meanwhile, in both DSMIL-CNT cathode and common bar electrode CNT ones, cathode electrons would derive from CNTs of the top emitter layer, which is consistent with the previous description (SEM photos in Figs.2(b, and d)). In the DSMIL-CNT cathode, due to the coverage by the top emitter layer fabricated on the particles-mixed CNT layer, the Ag particles would not appear on the cathode surface. To avoid a poor-performance parasitic electron emission of Ag particles and its interference with CNT ends'-produced one, the top emitter layer of the DSMIL-CNT cathode, which suppressed the electron emission from minute Ag particles, was designed and fabricated. This was consistent with the results of SEM analysis for the DSMIL-CNT cathode in Fig.2(b): typical “field emission” characteristics of both types of CNT cathodes confirmed that the emission current came from the CNT, rather than from the Ag particles. Secondly, seen from the changing strenuous degree of the experimental curve, the electron emission characteristics of the DSMIL-CNT cathode were superior to those of the common bar electrode CNT one. For example, at the initial stage of the curve, when the electric field intensity was enhanced from 2.12 to 2.39V/ μm , the increment of electron emission current for the DSMIL-CNT cathode was 240.6 μA , which exceeded that of the common bar electrode CNT cathode of 136.3 μA . Within the same electric field intensity interval of 0.27V/ μm , the difference of emission current increasing range for both types of CNT cathode was 104.3 μA . It was obvious that the emission current increasing range of the DSMIL-CNT cathode was large. Nevertheless, at the intermediate curve stage, when the electric field intensity was enhanced from 2.78 to 3.05V/ μm , the emission current increasing range of common bar electrode CNT cathode was 724.1 μA , which was less than that of DSMIL-CNT cathode of 1188.7 μA . Again, the electric field intensity interval was also 0.27V/ μm . However, the difference in emission current increasing range for the two CNT cathodes rose to 464.6 μA . The analysis shows that, in the DSMIL-CNT cathode, with the silver-CNT composite electrode, many CNTs and original silver slurry particles were included in silver-CNT composite electrode paste and underwent the printing, baking, and sintering processes. After the sintering process, the printed original silver slurry had been solidified, so the CNTs were embedded or semi-embedded into the silver-CNT composite electrode. This

improved the electric contact between the silver electrode and CNTs. The contact resistance was decreased greatly, and the transmission of electrons between the silver electrode and CNTs would be smoother. Moreover, for the semi-embedded CNTs in the silver-CNT composite electrode, one end was fixed on the silver electrode, while the other end was twined around with the CNTs in the top emitter layer or particles-mixed CNT layer. This contributed to enhancing the adhesive performance of CNTs: even under a strong electric field intensity, the CNTs would not fall-off easily. With the fabricated silver-CNT composite electrode, the cathode potential is required for good conductivity of the CNTs in top emitter layer; so, with the same electric field intensity interval, the increasing range in the emission current for DSMIL-CNT cathode is enhanced. Thirdly, according to the experimental curve's peak value trend, the DSMIL-CNT cathode possessed stronger electron emission capability. For example, with the same electric field intensity of $2.83\text{V}/\mu\text{m}$, the electron emission current of the DSMIL-CNT cathode was $1276.8\mu\text{A}$, while that of common bar electrode CNT cathode was only $926.7\mu\text{A}$; the difference of emission current for both types of CNT cathode was $350.1\mu\text{A}$. It was evident that the emission current of the DSMIL-CNT cathode was larger. On the contrary, for the same emission current of $1463.6\mu\text{A}$, the common bar electrode CNT cathode's required electric field intensity was $3.02\text{V}/\mu\text{m}$, exceeding that of DSMIL-CNT cathode ($2.87\text{V}/\mu\text{m}$). The difference in the required electric field intensity for both types of CNT cathode was $0.15\text{V}/\mu\text{m}$. Furthermore, the maximum emission current of the DSMIL-CNT cathode was $2915.7\mu\text{A}$, while that of the common bar electrode CNT cathode was $1773.5\mu\text{A}$. The analysis shows that Ag particles were added to the particles-mixed CNT layer, and the particle diameter of Ag particles was similar to that of CNTs. In the sintering course, numerous Ag particles penetrated the idle space of CNTs, and the vacuum among CNTs was occupied. On the one hand, after the sintering process, CNTs in the top emitter layer and particles-mixed CNT layers twined each other, the interface between the top emitter layer and the particles-mixed CNT layer would also disappear. Due to the efficient separating of Ag particles in dense CNTs, the electric field enhance factor was strongly improved, while the electric field shielding effect of adjacent CNTs was weakened. On the other hand, the Ag particles spread all over the silver-CNT composite electrode surface and were in close contact with the CNTs, which expanded the contact area between the CNTs and the silver electrode. The cathode electrons could emit more rapidly and, as a result, the electron emission current of the DSMIL-CNT cathode would be larger with the identical electric field intensity. Besides, in the DSMIL-CNT cathode, silver-CNT composite electrodes were fabricated over the transparent bar electrode. Due to the good electric conduction between the silver-CNT composite electrode and the transparent bar electrode, CNTs in the top emitter layer could reach the required level of cathode potential, which was beneficial for more intensive electron emission current. In one silver-CNT composite electrode, the circular convex shape on the outer electrode edges was designed. As compared to the transparent bar electrode, the electrode area of the DSMIL-CNT cathode was effectively increased, which implied that more

CNT ends would be prepared on the electrode surface. As more CNT ends were involved in the electron emission, it was advantageous that the large emission current was formed for the DSMIL-CNT cathode. As seen from Fig.3, the common bar electrode CNT cathode needs more intense electric field intensity to achieve the required emission current. These results were corroborated by the experimentally revealed increase in the emission current of the DSMIL-CNT cathode.

3.3 Emission current stability comparison

Emission current stability is one of the key technological indexes for evaluating the practical application of the DSMIL-CNT cathode [26-29]. The DSMIL-CNT cathode must provide a stable cathode current for a long time if the flat panel display could operate normally [30-33]. The emission current stability testing for DSMIL-CNT cathode and common bar electrode CNT cathode was carried out on an integrated vacuum measuring system platform. Both types of CNT cathodes were placed in a closed drying oven for idle placement of 24 h. Then, both types of CNT cathode were tested in a proper sequence, and the testing conditions were as follows: the measuring time was 120 min; the measuring process was continuous; the emission current was monitored with DC ammeter, and the initial emission current was set to 763.5 μ A; the measuring time interval was 3 min. The experimental curves of emission current stability for both types of CNT cathode are depicted in Fig.4.

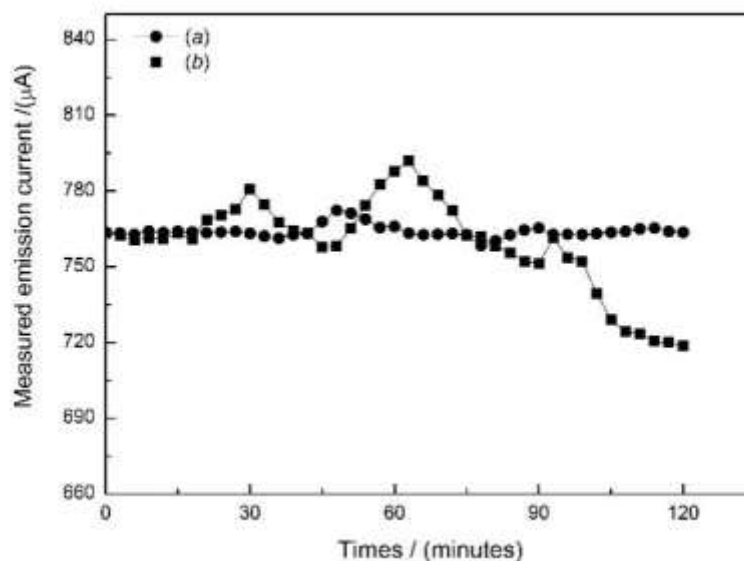


Fig 4: Experimental curves of emission current stability for (a) the DSMIL-CNT cathode, and (b) the common bar electrode CNT cathode.

As seen in Fig.4, (1) Comparing with the common bar electrode CNT cathode, the variation trend of emission current for the DSMIL-CNT cathode was more stable. In the measuring course, the rising and falling of emission current would exist for both types of CNT cathode. However, the fluctuation range of emission current for the DSMIL-CNT cathode would not exceed 1.2%. For the common bar electrode CNT cathode, at the former measuring stage (for example, the testing time range was 0~72 min), the maximum fluctuation range of emission current reached 4.5%; at the latter measuring stage (for example, the testing time range was 73~120 min), the maximum fluctuation range of emission current would exceed 5.9%. (2) As compared to the common bar electrode CNT cathode, the DSMIL-CNT one possessed a more persistent emission current. In the measuring course of 120 min, the strong electron emission capability was maintained for the DSMIL-CNT cathode, in which the rising and falling ranges of emission current were smaller. However, after idle placement of 24 hours, the emission current value was not significantly decreased. For the common bar electrode CNT cathode, a proper emission current could be preserved in the former measuring stage. Yet, at the latter measuring stage, the electron emission current decreased significantly with the extension of measuring time, and the rebound trend to the proper emission current did not appear. Given the above findings, the emission current stability of the DSMIL-CNT cathode was superior. In DSMIL-CNT cathode, the silver-CNT composite electrode was fabricated, in which the cathode potential could be conducted rapidly, the CNT ends could be effectively increased, and the contact resistance between the silver electrode and CNTs could be reduced; the particles-mixed CNT layer was also prepared, of which the adhesive performance of CNTs could be significantly enhanced. So, the DSMIL-CNT cathode could possess more reliable and stable electron emission.

3.4 Emission images comparison

Utilizing the integrated vacuum measuring system platform, the application effectiveness of the DSMIL-CNT cathode was tested. The common experimental anode faceplate and correlated components were first fixed in the vacuum chamber of the integrated vacuum measuring system platform, and multiple DSMIL-CNT cathodes were arranged and assembled behind the common experimental anode faceplate; the gas in the vacuum chamber was evacuated to form a vacuum environment. Whether the emission image luminescence could be realized was an appropriate and expeditious method to predict the application effectiveness of the DSMIL-CNT cathode. Fig.5 presents a group of real testing photos in the experiment. The green phosphor was prepared on the experimental anode faceplate, so the green luminescence of image pixels could be achieved. Since the electron emission abilities of each DSMIL-CNT cathodes were different, there were also differences in the luminous brightness for image pixels on the

common experimental anode faceplate. If the image pixels had been illuminated and the luminous brightness was high, the corresponding DSMIL-CNT cathode's application effectiveness would be superior, and the corresponding DSMIL-CNT cathode was also suitable for the packaging in flat panel display. If some image pixels were almost non-luminous, or the luminous brightness of other image pixels was low, the application effectiveness of those corresponding DSMIL-CNT cathodes was poor, and the latter cathodes should be directly rejected.

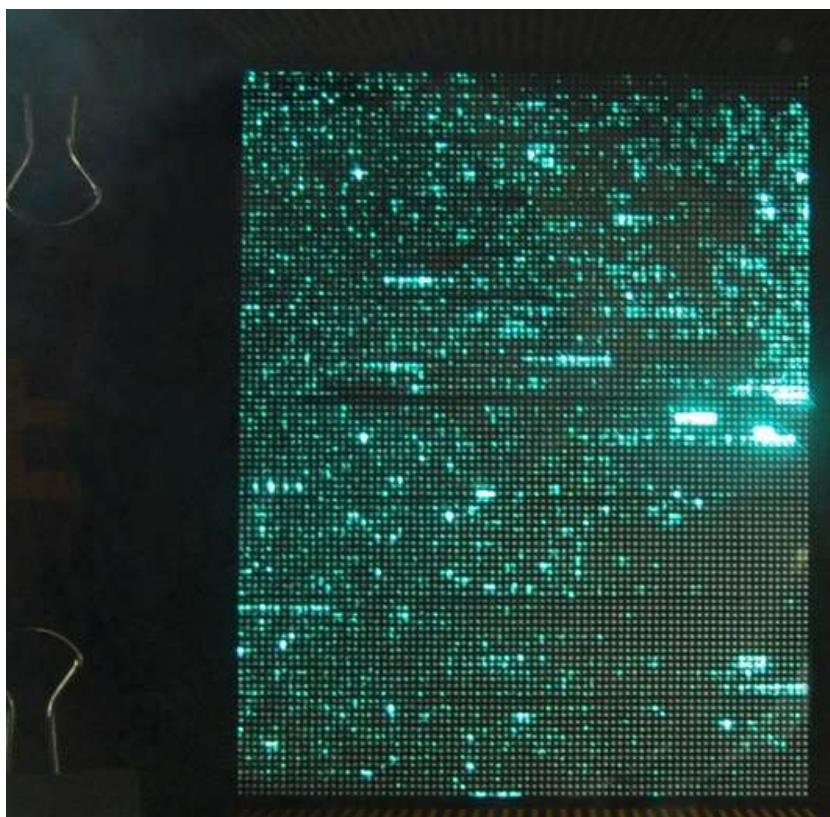


Fig 5: Real testing photos of application effectiveness for the DSMIL-CNT cathode.

Using the DSMIL-CNT cathode with good application effectiveness, a flat panel display sample was fabricated. The horniness cathode faceplate and the horniness anode faceplate were used to constitute the vacuum room. After the exhaust process, the packaged DSMIL-CNT cathode was located in the vacuum environment. A photo of a flat panel display with DSMIL-CNT cathode is presented in Fig.6(a). As seen from the photo, the flat panel display's image pixels were on the horniness anode faceplate. Due to the covering of the horniness anode faceplate, the DSMIL-CNT cathode was invisible from the flat panel display. The horniness cathode faceplate was both the vacuum room's outer shell and the substrate of the DSMIL-CNT cathode. After the proper bias voltage were applied, image pixels' image luminescence for flat

panel display appeared. The electron emission current could be monitored with ammeter, and good electron emission characteristics would also be demonstrated. This implies that the DSMIL-CNT cathode fabrication was feasible. Utilizing a common bar electrode CNT cathode, the corresponding flat panel display with a similar manufacturing structure was also fabricated, in which the only difference was that the DSMIL-CNT cathode was replaced. The emission image of the common bar electrode CNT cathode is shown in Fig.6(b), and that of DSMIL-CNT cathode is illustrated in Fig.6(c). As seen from the emission images, both types of CNT cathode could provide cathode electrons to form the cathode current, and the emission image was also formed. The luminous brightness of image pixels was appropriate, which also indicated that the number of cathode electrons generated by both types of CNT cathode was sufficient. The comparative analysis of the two emission images revealed significant differences in their technical specifications, including the luminous brightness and luminescence uniformity. In Fig.6(b), the luminous brightness of image pixels was not homogeneous; the luminous brightness of different image pixels varied greatly. Moreover, some image pixels would not generate visible light at all. However, in Fig.6(c), all the image pixels' luminescence was uniform, and the luminous brightness was also quite high. Due to higher luminous brightness, the center of some image pixels became white, with green tints around the image pixel. The luminescence of all the high-brightness image pixels was visible in daylight. The above findings strongly indicate that the developed DSMIL-CNT cathode possessed excellent electron emission performance and application effectiveness.



(a)

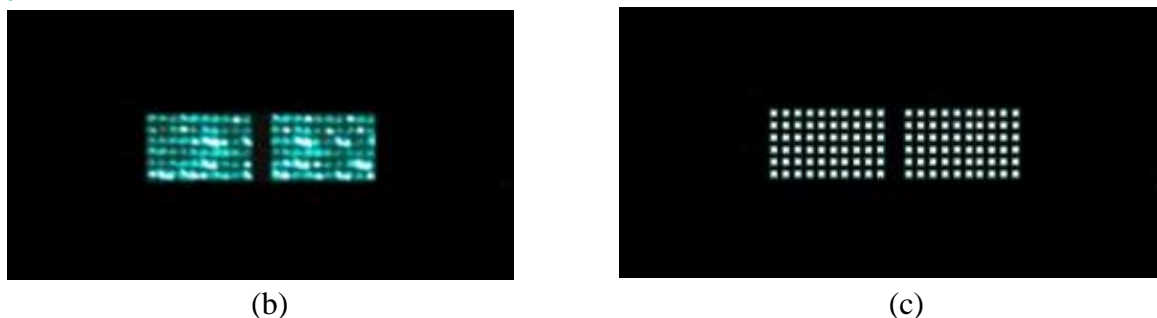


Fig 6: (a) Real photo of flat panel display with DSMIL-CNT cathode, (b) emission image of the common bar electrode CNT cathode, and (c) emission image of the DSMIL-CNT cathode.

IV. CONCLUSIONS

Feasibility studies on the fabrication of DSMIL-CNT cathodes for practical applications were performed. The DSMIL-CNT cathode consisted of four layers, in which the transparent bar electrode, silver-CNT composite layer, particles-mixed CNT layer, and top emitter layer were included. CNTs in the top emitter layer were the main cathode electron sources. The cathode potential applied to the transparent bar electrode could be conducted with the introduced silver-CNT composite electrode and particles-mixed CNT layer. The conventional screen-printing, baking, and sintering processes also contributed to the low-cost fabrication of the DSMIL-CNT cathode. The emission current of the DSMIL-CNT cathode was not significantly reduced during the continuous operation for up to 120 min, which confirmed the excellent emission current stability of the DSMIL-CNT cathode. The fabricated DSMIL-CNT cathode possessed superior electron emission characteristics and good adhesive performance, which also indicated that it was a good optional approach of improving the electron emission performance of screen-printed CNTs. When the electric field intensity was enhanced from 2.12 to 2.39V/ μm at the initial testing curve stage, the emission current increasing range of the DSMIL-CNT cathode was 240.6 μA . At the testing curve intermediate stage, when the electric field intensity was enhanced from 2.78 to 3.05V/ μm , the increment of emission current was widened to 1188.7 μA . The maximum electron emission current for the DSMIL-CNT cathode was 2915.7 μA . The emission image of the DSMIL-CNT cathode, with good luminance uniformity and high luminous brightness, could be successfully achieved. The fabrication of the DSMIL-CNT cathode would advance commercial flat panel displays and their practical applications.

ACKNOWLEDGEMENTS

This research was supported by Project supported by the National Natural Science Foundation of China (No.61302167) and the Scientific Research Starting Foundation for High Level Talents in Jinling Institute of Technology (No.jit-rcyj-201602).

REFERENCES

- [1] Lucian D. Filip, Valeriu Filip. Influence of electron quantum confinement on the strength of carbon nanotube bundles [J]. *Solid State Electronics Letters*, 2019, 1(1): 1-9.
- [2] Danial Danaei, Amir Abbas Nourbakhsh, Parvaneh Asgarian, et al. Synthesis of nanosized SiC by low-temperature magnesiothermal reduction of nanocomposites of functionalized carbon nanotubes with MCM-48 [J]. *Ceramics International*, 2019, 45(5): 5525-5530.
- [3] Gwan Woo Kim, Gunn Kim. Behavior of H₂O molecule in carbon nanotube /boron nitride nanotube heterostructure [J]. *Current Applied Physics*, 2019, 19(6): 675-678.
- [4] Amara Arshad, Ayesha Taj, Abdul Rehman, et al. In situ synthesis of highly populated CeO₂ nanocubes grown on carbon nanotubes as a synergy hybrid and its electrocatalytic potential [J]. *Journal of Materials Research and Technology*, 2019, 8(6): 5336-5343.
- [5] Laura M. Esteves, Andressa A. Daas, Hugo A. Oliveira, et al. Influence of space velocity and catalyst pretreatment on CO_x free hydrogen and carbon nanotubes production over CoMo/ MgO catalyst [J]. *International journal of hydrogen energy*, 2020, 45(51): 27299-27311.
- [6] Narasingh Deep, Punyapriya Mishra. Evaluation of mechanical properties of functionalized carbon nanotube reinforced PMMA polymer nanocomposite [J]. *Karbala International Journal of Modern Science*, 2018, 4(2): 207-215.
- [7] Roya Mahinpour, Leila Moradi, Zohreh Zahraei, et al. New synthetic method for the synthesis of 1,4-dihydropyridine using aminated multiwalled carbon nanotubes as high efficient catalyst and investigation of their antimicrobial properties [J]. *Journal of Saudi Chemical Society*, 2018, 22(7): 876-885.
- [8] Obid Tursunov, Zaid Tilyabaev. Hydrogenation of CO₂ over Co supported on carbon nanotube, carbon nanotube-Nb₂O₅, carbon nanofiber, low-layered graphite fragments and Nb₂O₅ [J]. *Journal of the Energy Institute*, 2019, 92(1): 18-26.
- [9] Nur Syazana Anuar, Norfifah Bachok, Mustafa Turkyilmazoglu, et al. Analytical and stability analysis of MHD flow past a nonlinearly deforming vertical surface in carbon nanotubes [J]. *Alexandria engineering journal*, 2020, 59(1): 497-507.
- [10] Lina Marcela Hoyos-Palacio, Diana Paola Cuesta Castro, Isabel Cristina Ortiz-Trujillo, et al. Compounds of carbon nanotubes decorated with silver nanoparticles via in-situ by chemical vapor deposition (CVD) [J]. *Journal of Materials Research and Technology*, 2019, 8(6): 5893-5898.
- [11] Chi-Jung Chang, Yi-Hung Wei, Wen-Shyong Kuo. Free-standing CuS-ZnS decorated carbon nanotube films as immobilized photocatalysts for hydrogen production [J]. *International Journal of Hydrogen Energy*, 2019, 44(58): 30553-30562.
- [12] G. Satish, V.V.S. Prasad, Koona Ramji. Effect on mechanical properties of carbon nanotube based composite [J]. *Materials Today: Proceedings*, 2018, 5(2): 7725-7734.

- [13] Elisabeth Abbe, Thomas Renger, Maciej Sznajder, et al. A material experiment for small satellites to characterise the behaviour of carbon nanotubes in space – development and ground validation [J]. *Advances in Space Research*, 2019, 63(7): 2312-2321.
- [14] Bin-Hao Chen, Chieh Kung. Quantum confinement and torsional responses of single-wall carbon nanotubes filled with hydrogen molecules [J]. *International journal of hydrogen energy*, 2020, 45(58): 33798-33806.
- [15] T. Nagaraj, A. Abhilash, R. Ashik, et al. Mechanical behavior of carbon nanotubes reinforced AA 4032 bimodal alloys [J]. *Materials Today: Proceedings*, 2018, 5(2): 6717-6721.
- [16] Shrilekha V. Sawant, Seemita Banerjee, Ashwin W. Patwardhan, et al. Effect of in-situ boron doping on hydrogen adsorption properties of carbon nanotubes [J]. *International Journal of Hydrogen Energy*, 2019, 44(33): 18193-18204.
- [17] Vilas G. Dhore, W.S. Rathod, K.N. Patil. Synthesis and characterization of high yield multiwalled carbon nanotubes by ternary catalyst [J]. *Materials Today: Proceedings*, 2018, 5(2): 3432-3437.
- [18] Pankaj Kumar Tripathi, Anil Kumar, Kamal Kumar Pandey. Dielectric study of multiwall carbon nanotube dispersed nematic liquid crystal mixture [J]. *Materials Today: Proceedings*, 2018, 5(3): 9182-9186.
- [19] Phongnared Boontueng, Sittipong Komin. Theoretical study of ethanol interaction with pristine and P-doped single-walled carbon nanotubes [J]. *Materials Today: Proceedings*, 2018, 5(5): 11043-11050.
- [20] Fatih Selimefendigil. Mixed convection in a lid-driven cavity filled with single and multiple-walled